Journal of Power Sources 657 (2025) 238177

Contents lists available at ScienceDirect

Journal of Power Sources

journal homepage: www.elsevier.com/locate/jpowsour

# Scaling up pullulan-based supercapacitors: A sustainable approach to binder and separator integration in EDLCs

Elisabetta Petri [a,b], Maria Arnaiz [c], Chiara Gualandi [a,d,e], Francesca Soavi [a,b,d,*], Jon Ajuria [c,**]

[a] Department of Chemistry "Giacomo Ciamician", Alma Mater Studiorum University of Bologna, Via Piero Gobetti, 85, 40129, Bologna, Italy
[b] Center for the Environment, Energy, and Sea - Interdepartmental Centre for Industrial Research in Renewable Resources, Environment, Sea and Energy (CIRI-FRAME), Alma Mater Studiorum University of Bologna, Viale Ciro Menotti, 48, Marina di Ravenna, 48122, RA, Italy
[c] Centre for Cooperative Research on Alternative Energies (CIC energiGUNE), Basque Research and Technology Alliance (BRTA), Alava Technology Park, Albert Einstein 48, 01510, Vitoria-Gasteiz, Spain
[d] National Reference Center for Electrochemical Energy Storage (GISEL) - INSTM UdR of Bologna, Via G. Giusti 9, 50121, Firenze, Italy
[e] Interdepartmental Center for Industrial Research on Advanced Applications in Mechanical Engineering and Materials Technology, CIRI-MAM, University of Bologna, Viale Risorgimento, 2, 40136, Bologna, Italy

## HIGHLIGHTS

- Water-processable pullulan as dual binder and separator in EDLCs.
- Scaled pouch cells with ≥5 mg cm$^{-2}$ electrodes, 8 wt% binder content.
- Pouch cells (20 cm$^2$, 4 F) validated with ACN and greener PC electrolytes.
- PC-based cells outperform ACN at 60 °C, enabling safer high-T operation.
- Fully water-processed EDLCs shown viable for sustainable large-scale production.

## GRAPHICAL ABSTRACT

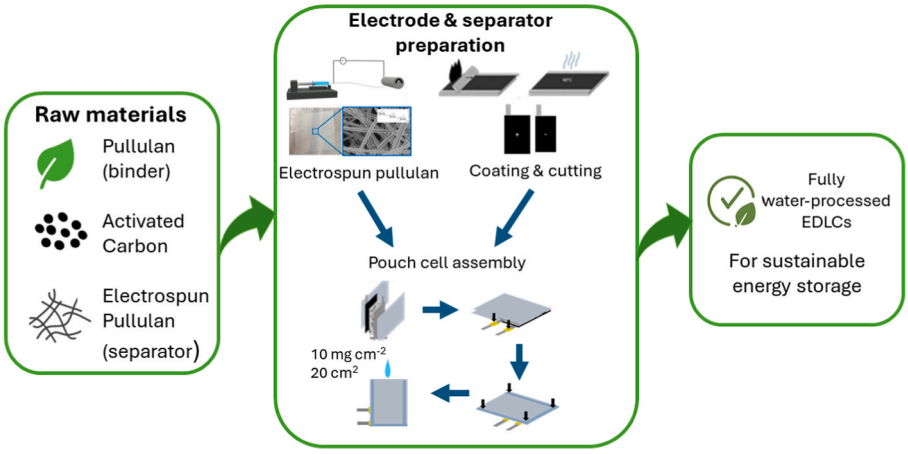


## ARTICLE INFO

*Keywords:*
Supercapacitors
Pullulan
Electrospun separators
Water processable electrodes and separator
Biopolymer

## ABSTRACT

Electrochemical double-layer capacitors (EDLCs) play a critical role in high-power energy storage, offering exceptional durability and longevity for diverse applications. EDLCs typically utilize activated carbon electrodes combined with organic electrolytes, produced through cost-effective roll-to-roll manufacturing, and achieving operating voltages of approximately 2.7 V. Replacing toxic materials in electrode fabrication is critical for transitioning towards sustainable manufacturing practices. A key component in their production is the binder,

* Corresponding author. Department of Chemistry "Giacomo Ciamician", Alma Mater Studiorum University of Bologna Via Piero Gobetti, 85, 40129 Bologna, Italy.
** Corresponding author.
*E-mail addresses:* francesca.soavi@unibo.it (F. Soavi), jajuria@cicenergigune.com (J. Ajuria).

https://doi.org/10.1016/j.jpowsour.2025.238177
Received 4 July 2025; Received in revised form 3 August 2025; Accepted 18 August 2025
Available online 26 August 2025

which must ensure uniform coating, thermal and mechanical stability, optimal microstructural properties, electrochemical inertness, and environmentally friendly processing. Pullulan (PUL), a water-soluble polysaccharide, emerges as a promising alternative, offering reduced environmental impact and cost benefits. Our recent studies demonstrated the feasibility of PUL as a binder for aqueous processed EDLCs at the laboratory-scale. However, scaling up this process and validating it for large-scale EDLC electrodes remain open challenges. Here, we present a comprehensive investigation into the optimization of low-binder-content, high-mass-loading electrode manufacturing at both laboratory and pre-industrial scales. Moreover, a PUL electrospun membrane has been also investigated as separator. The optimized electrode formulations are validated in pouch cells with 20 $cm^2$ electrodes, providing critical insights into the feasibility and scalability of the proposed supercapacitor configuration.

## 1. Introduction

Our society faces the significant challenge of transitioning from fossil fuels that induce global warming, such as oil, coal, and gas, to renewable and more sustainable alternatives like solar and wind power. Due to the inherent intermittency and often decentralized nature of these renewable sources, efficient and sustainable energy storage has become critically important. Electrochemical energy storage technologies, including secondary batteries and electrochemical double-layer capacitors (EDLCs), are considered among the most suitable options, particularly for applications such as transportation and short- to mid-term stationary energy storage. Batteries and EDLCs are pivotal in advancing towards a sustainable energy future [1,2].

While batteries store energy through diffusion-limited faradaic reactions to achieve high energy, EDLCs store energy through the rapid and reversible electrostatic adsorption of ions into porous electrode materials, offering high power and enhanced durability. Commercial EDLCs commonly employ activated carbon (AC) electrodes paired with organic electrolytes, operate at approximately 2.7 V, and are manufactured using highly efficient roll-to-roll processes [3,4].

A critical component in the production of EDLCs is the binder, which must meet various stringent criteria. It must enable uniform coating onto the aluminium current collector with the proposed carbon, while demonstrating thermal stability and mechanical robustness to withstand high drying temperatures without changing its binder properties. Additionally, it must preserve the integrity of the electrode coating throughout manufacturing processes, such as bending and rolling. On a microscopic scale, the binder plays a vital role in ensuring an optimal electrode structure, facilitating the dispersion of conductive additives, minimizing electrical resistance, and avoiding interference with the electrochemical performance of the device [5]. Importantly, to align with sustainable manufacturing goals and looking to easily recyclable methods, the binder should be processable in an environmentally friendly way [6,7].

Nowadays, poly(vinylidene fluoride) (PVDF) is the most commonly used binder for organic electrolyte systems, enabling the production of high mass loading electrodes (>10 mg $cm^{-2}$) for the development of commercial electrodes. The conventional PVDF-based electrode manufacturing process depends on N-methyl-2-pyrrolidone (NMP) as a solvent/dispersant, despite its toxic properties. The drying phase, which requires high temperatures to evaporate NMP (b.p 202 °C), represents one of the most energy-intensive steps in electrode production. Additionally, the complexity and costs associated with recovering NMP further exacerbate the environmental impact. Moreover, NMP itself is recognized as mutagenic and teratogenic, raising health and environmental concerns [7–13]. Adopting aqueous electrode processing methods and replacing toxic components with eco-friendly alternatives are crucial steps toward achieving sustainable and environmentally responsible energy storage technologies [7]. Carboxymethyl cellulose (CMC) currently represents the state-of-the-art aqueous, non-fluorinated binder for EDLCs. However, its limitations, such as cracking during the drying process and reduced flexibility at mass loadings higher than 5 mg $cm^{-2}$, remain significant challenges [7,14]. Over the past decade, numerous green alternative electrode and electrolyte components have been proposed [15–18]. These alternatives have shown promising material-level performance; however, they have been predominantly tested in lab-scale cells [4]. In this context, other water-soluble binders, such as pullulan (PUL), have emerged as promising alternatives with the potential to significantly reduce costs and environmental impact [19–23]. PUL is a natural water-soluble polysaccharide produced by the fungus *Aureobasidium pullulans fermentation*. Widely available, cost-effective, and neutral, PUL, owing to its numerous hydroxyl groups, forms extensive intermolecular hydrogen bonds, which make it highly soluble in water and hydrophilic, while it is insoluble in organic solvents [24]. This structural characteristic allows for the easy formation of fibers and films, which exhibit high thermal stability owing to high decomposition temperature (250–280 °C) [25]. However, its brittleness and hydrophilic nature can reduce the mechanical strength of the polymer. Recent studies show that the addition of glycerol (Gly) as a plasticizer enhances pullulan flexibility and durability, making it more suitable for EDLC [19–23,26]. Currently, PUL is more expensive than conventional fossil-based binders due to higher production costs, as is the case for most bio-based and natural polymers. However, a more meaningful cost comparison should consider not only the price of the binder itself but also the cost of all components of the slurry used for electrode coating, including the solvent. In our previous work [20], we have demonstrated that for PVDF-based electrode slurries, the major cost comes from NMP that is needed to solubilize the polymer. Instead, PUL-based slurries are aqueous. Hence, at present, while PUL is more expensive than PVDF, the corresponding ink formulations might be 70 % cheaper. At present PUL is more expensive than CMC, but its increasing market in sectors like pharmaceutical and cosmetic industries, is forecasting a significant cost reduction. Beyond its role as a binder, pullulan can also work as a separator in EDLCs. Indeed, self-standing, non-woven mats can be easily produced by electrospinning aqueous pullulan solutions [21]. Electrospinning, an established technique for producing nanofiber-based separators with meso- and macroporous structures, enables the fabrication of ultrathin fibers with high porosity, excellent structural stability, and liquid retention, which has already been proven effective in the battery field [22,27,28]. Electrospinning with PUL-based solutions offers a scalable method for manufacturing advanced separators [29]. In our previous work [19], we demonstrated that PUL electrospun separators not only represent a sustainable alternative to conventional materials but also exhibit superior electrochemical and thermal performance compared to cellulose-based (cellulose triacetate, CTA) counterparts. Electrochemical Impedance Spectroscopy (EIS) carried out at different temperatures showed that the McMullin number of PUL membranes in an imidazlium ionic liquid was lower than the value measured for CTA membranes. This was attributed to the thinner fiber diameter of PUL (~0.3 μm vs. ~0.6 μm for CTA), which increased the free volume accessible to ions and enhanced conductivity. Moreover, resistance values of the cells with PUL membrane remained stable over time and showed full reversibility after thermal aging at 60 °C, whereas the resistance of those with CTA membranes doubled and did not recover upon cooling. In addition, from a sustainability perspective, PUL offers significant advantages in terms of processing. While electrospinning CTA requires toxic solvents such as dichloromethane mixtures, which are carcinogenic and environmentally hazardous, PUL can be

electrospun directly from aqueous solutions, enabling safer and greener large-scale manufacturing. These combined performance and environmental advantages motivated us to further explore the potential of PUL for integrated use as both binder and separator in EDLCs. Despite promising results at the material level, translating the use of PUL as binder and separator components into scalable technologies remains challenging. Using green EDLC components should also ensure key performance improvements, like (i) reducing internal resistance, (ii) achieving high cyclability with coulombic efficiencies above 99 %, and (iii) maintaining high energy and power outputs. Furthermore, meeting industrial standards for activated carbon content (90–95 %) and mass loading (~10 mg $cm^{-2}$) in prototype electrodes is essential for designing high-energy EDLCs [22]. Therefore, optimizing electrode manufacturing parameters, ensuring morphological and mechanical quality by using industry-compatible tools, and validating electrochemical performance at the pouch cell level are critical for assessing the convenience of using PUL.

In this work, the assessment of PUL as both a binder and a separator has been conducted at the prototype level. First, a comprehensive study on the optimization and scale up of water-processable electrode manufacturing process was conducted, focusing on minimum usage of binder and maximum loading output. This initial phase included slurry preparation by mixing active materials, conductive additives, and binders, followed by casting using a doctor blade. Electrode quality and mechanical stability were evaluated through cross-sectional and top-view SEM analysis, bending tests, and validated through electrochemical characterization in small lab cells (1.13 $cm^2$). Then, the most promising formulation was scaled up to a pilot production level by increasing the volume, adjusting the equipment and its operating parameters. As a result, electrodes with low amount of pullulan (4 wt%) and high mass loading (10 mg $cm^{-2}$) were achieved, equalling electrodes with industry standards. Second, the resulting electrodes were combined with PUL electrospun separator to evaluate the complete system in monolayer pouch cells. At this stage, the performance of PUL-based EDLCs featuring electrolytes formulated with tetramethylammonium tetrafluoroborate ($Et_4NBF_4$) in acetonitrile (ACN) and propylene carbonate (PC) were evaluated. While ACN serves as the benchmark solvent, PC is considered a more sustainable, less toxic alternative. Finally, to assess their performance, a comprehensive electrochemical characterization was conducted to validate the use of PUL as a binder, investigate the impact of different electrolytes, and explore the application of PUL electrospun membranes as separators. A threshold criterion balancing performance and sustainability is applied in the evaluation process. The results highlight the potential of scaling up this approach to roll-to-roll electrode manufacturing, providing valuable insights into the performance and feasibility of these novel supercapacitor design.

## 2. Materials and methods

### 2.1. Electrode preparation

For the lab-scale investigation, electrode formulations were prepared using a high-performance dispersion-homogenizer (T 25 digital ULTRA-TURRAX®). The first step of slurry production involved dispersing the binder, Pullulan (PUL, Tokio Chemical Industry), in water at a fixed concentration (3.6 wt %) followed by 5 min of high shear mixing (HSM) at 16000 rpm. The conductive additive, Carbon black (C-ENERGY™ SUPER P C45, Imerys) was then added to the binder solution and stirred for 10 min using HSM at 16000 rpm. A commercial activated carbon (AC, YP-50F, Kuraray) was added and amalgamated by hand mixing, followed by 15 min of HSM stirring at 16000 rpm. Slurry formulations containing 70 wt%, 88 wt% and 91 wt% of AC, 20 wt%, 8 wt% and 6 wt % of binder and 10 wt%, 4 wt% and 3 wt% of C45 were prepared at lab-scale level and named sPUL-AC70, sPUL-AC88 and sPUL-AC91, respectively. At the scaling up phase, electrode production was achieved by the preparation of the slurry using a homogenizer (Dissolver DISPERMAT, VMA Getzman, Getzman), coupled with a chilling unit in order to maintain a constant temperature of 20 °C throughout the process. The first step of slurry production involved dispersing the binder in the water at the proper concentration followed by 45 min homogenization at 700 rpm. Carbon black (C-ENERGY™ SUPER P C45, Imerys) was then added to the binder solution and mixed for 60 min at 1000 rpm. Activated carbon (AC, YP-50F, Kuraray) was slowly added next, followed by 90 min of mixing at 1800 rpm. In this paper, slurry formulations containing 70 wt% and 88 wt% of activated carbon, 20 wt% and 8 wt% of binder and 10 wt% and 4 wt% of carbon black were prepared and named dPUL-AC70 and dPUL-AC88, respectively.

Electrode slurries were casted on carbon-coated aluminium current collectors (ARMOR) using a doctor blade film applicator, dried at room temperature (RT) for 2 h followed by oven drying at 60 °C overnight before being punched. Different wet thicknesses were applied to achieve the desired mass loadings (150, 200, 250, 300 μm), reaching single electrode mass loading of 2–11 mg $cm^{-2}$.

### 2.2. Electrospun pullulan membrane production

The electrospun membrane was produced using a home-made electrospinning machine, which included a high-voltage power supply (SL 50 P 10/CE/230, Spellman, West Sussex, UK), a syringe pump (200 series, KD Scientific, Holliston, MA, USA), and a glass syringe containing the polymer solution [30,31]. The syringe was connected to a stainless-steel blunt-ended needle (inner diameter = 0.51 mm) via a polytetrafluoroethylene (PTFE) tube. The PUL membrane was electrospun from a 23 % w/v solution of the polymer in Milli-Q water. The solution was electrospun at 18 kV, with the collector positioned 20 cm away from the needle, and a flow rate of 1 mL $h^{-1}$. The obtained PUL electrospun membrane had a thickness in the range 80–120 μm.

### 2.3. Electrolytes preparation

Electrolyte solutions were composed of 1 M tetra alkyl ammonium tetrafluoroborate ($Et_4NBF_4$, >99 %, Sigma Aldrich) in acetonitrile (ACN) or Propylene Carbonate (PC, FUJI FILM). The $Et_4NBF_4$ - ACN solution was purchased from E-Lyte Innovation and used as received. In the case of the $Et_4NBF_4$ - PC solution, the salt was added to the solvents and was left to dissolve under stirring overnight. All procedures were performed in an Ar-filled glovebox ($O_2$ < 0.1 ppm; $H_2O$ < 0.1 ppm, McBraun).

### 2.4. Cell assembly

Swagelok cells were assembled in an Ar-filled glovebox ($O_2$ < 0.1 ppm; $H_2O$ < 0.1 ppm, McBraun) using a two-electrode symmetric configuration with an electrode area of 1.13 $cm^2$. The mass ratio between the positive and negative electrodes is 1.1:1 ($AC^+$:$AC^-$). Glass fiber membranes (Whatman™ GF/D) were used as separators, and tetra alkyl ammonium tetrafluoroborate in acetonitrile (1M $Et_4NBF_4$ ACN, purchased from E-Lyte Innovation) was used as the electrolyte. Finally, the cells were placed under pressure using clamps.

Then, pouch cells were assembled with PUL-based electrodes made with the best formulation, namely AC:PUL-Gly:C45 = 88:8:4, obtained by high-speed disk mixer and doctor blade casting (the resulting electrode was named dPUL-AC88). Monolayer pouch cells were assembled at 21 °C into an ISO class 7 dry room with an average dew point of −60 °C and 21 °C and 30 Pa overpressure. Monolayers of ca. 20 $cm^2$ of electrode area using a single PUL electrospun membrane as separator were assembled. The mass ratio between the positive and the negative electrode is of 1.1 ($AC^+$:$AC^-$). Either 1 M $Et_4NBF_4$ in ACN or 1 M $Et_4NBF_4$ in PC was used. Pouch cells were compressed under a torque of 2 N m between stainelss steel plates to ensure good contact and minimize internal resistance.

### 2.5. Physical characterization

The flexibility of the fabricated electrodes (from high-speed mixer slurries) was studied by bending tests using Elcometer 1506-B Cylindrical Mandrel Bend Tester. The frame features a bending lever with height-adjustable rollers and a sliding vice for clamping the sample. Mandrels with diameters of 32, 25, 20, 16, 12, 8, 5, 3, and 2 mm were used until cracks appeared in the laminates, indicating the maximum bend that the material can undergo. Sample preparation for the cross-section study of the electrodes was performed on a Hitachi 4000 Plus ion milling, which utilizes a broad, low-energy $Ar^+$ ion beam (0–6 kV acceleration voltage) milling method. The microstructure of the laminates was analyzed by scanning electron microscopy (SEM) and energy dispersive spectroscopy (EDX) utilizing a FEI Quanta 200 field-emission gun SEM.

### 2.6. Electrochemical characterization

The electrochemical tests were performed at RT and at 60 °C using a multichannel VMP3 Bio-Logic potentiostat/galvanostat. Pouch cells were tested by a multichannel BT-Lab potentiostat/galvanostat capable of handling high currents.

To evaluate the full cell impedance, EIS in two-electrode configurations were performed before and after the complete electrochemical test, under open circuit conditions, with a frequency range of 10 kHz – 10 mHz and 50 mV alternating current perturbation, acquiring 6 points per decade.

Nyquist plots have been analyzed referring to the equivalent circuit described in the Supplementary Information, and according to Equation (1) for calculating capacitance from impedance:

$$C(f) = \frac{-1}{2\pi f Z_{im}(f)} \quad (1)$$

where C is expressed in Farad (F), $f$ is the lowest frequency applied expressed in Hertz and $Z_{im}$ is the imaginary part of the impedance corresponding to the lowest frequency expressed in Ohm, as the imaginary part of the impedance $Z_{im}(f)$ increases at lower frequencies, the calculated capacitance decreases. This inverse relationship highlights how larger impedance values, particularly at low frequencies, correspond to a reduction in the overall capacitance of the system.

Cyclic voltammetries (CVs) were run at different scan rates of 10, 20, 50, 100, and 200 mV $s^{-1}$ between 0.0 V and 2.7 V. CV were analyzed to get a preliminary evaluation of the EDLC-specific capacitance ($C^{sp}_{EDLC}$). Specifically, $C_{EDLC}$ (F $g^{-1}$) was calculated by dividing the positive value of the current point by point by the respective scan rate and normalizing by the total composite mass of the two electrodes or the electrode's area.

Then, constant current tests were performed, consisting of galvanostatic charging up to 2.7 V followed by a holding time of 5 s for charge stabilization and galvanostatic discharging to 0 V. Galvanostatic charge-discharge (GCD) rate capability tests were performed at different specific currents for Swagelok cells (0.1, 0.25, 0.5, 1, 2, 3, 5, 7, 10, 20, 50 A $g^{-1}$) and at different currents for pouch cells (0.1, 0.2, 0.5, 1, 2, 3, 5, 10 A) between 0.0 V and 2.7 V. The GCD curves were analyzed to quantify the discharge time, equivalent series resistance (ESR), $C^{sp}_{EDLC}$ and the specific energy and power of the devices at different discharge currents. The discharge time ($t_{dis}$) was calculated according to Equation (2), where $t_0$ is the time before the discharge after 5 s of floating at the maximum potential (2.7 V), $t_f$ is the time after the galvanostatic discharge:

$$t_{dis} = (t_0 - t_f) \quad (2)$$

ESR was calculated according to Equation (3), where $\Delta V_{ohmic}$ is the ohmic voltage drop at the beginning of discharge, and i is the current (A):

$$ESR\ [\Omega] = \Delta V_{ohmic} / i \quad (3)$$

$C^{sp}_{EDLC}$ was calculated by multiplying the current density by the discharge time and dividing by the potential escursion after the ohmic drop (Vi) down to 0 V, according to Equation (4):

$$C^{sp}_{EDLC}\ [F\ g^{-1}] = i \cdot t_{dis} / V_i \quad (4)$$

The EDLC-specific energy (E) and power (P) were calculated from the GCPL discharge curves through Equations (5) and (6):

$$E\ [Wh\ kg^{-1}] = (½\ C^{sp}_{EDLC}\ V_i^2 / 3.6) \quad (5)$$

$$P\ [W\ kg^{-1}] = 3600 \times E / t_{dis} \quad (6)$$

The stability of the devices assembled in pouch cells was assessed through accelerated aging tests, specifically using floating experiments. Initially, the cell was held at open circuit voltage (OCV) for 1 h. Then, it underwent a galvanostatic charge at 1 An until reaching 2.7 V, after which it was held at 2.7 V for 5 s, and discharged galvanostatically. This cycle was repeated 10 times to evaluate the capacitance retention of the system. Subsequently, the cell was charged to 2.7 V at 1 A and held at this voltage for 10 h. This entire procedure was repeated continuously for a total of 1000 h to evaluate the long-term stability of the device, first at RT and then at 60 °C.

## 3. Results and discussion

The large-scale fabrication and optimization of pouch cells with water-processable electrodes using PUL as a binder is presented. A high-performance dispersion-homogenization approach was employed to maximize the AC content while minimizing the binder amount, targeting formulations compatible with scalable manufacturing processes. Electrodes with an active area of 20 $cm^2$ and single-side mass loadings of approximately 5 mg $cm^{-2}$ were assembled into pouch cells and subjected to a comprehensive electrochemical evaluation to validate the optimized formulation and assess the feasibility of their application in real devices. Notably, PUL, the biopolymer used as a binder, was also employed as a separator in the form of an electrospun membrane, enabling a fully bio-based and water-processable electrode/separator system.

### 3.1. Optimization of electrode formulation for large-scale manufacturing

The first part of the work focused on the optimization of the formulations of the aqueous slurry featuring PUL binder for electrode production at lab-scale. Slurries were prepared using a rotor-stator high-shear homogenizer which enables efficient dispersion of solid components in conditions closer to those encountered in industrial mixing processes, such as with the high-speed mixer. The aim was to explore the effect of increasing AC content and reducing binder content, while ensuring slurry homogeneity and adequate viscosity for electrode casting. Table 1 reports the most representative formulations, all prepared with a total solid mass of 2 g. These include slurries with 70 wt%, 88 wt %, and 91 wt% AC, with 20 wt%, 8 wt% and 6 wt% binder (PUL-Gly)

**Table 1**
Formulations of slurries with 2 g of solids (C45 and AC) prepared by high-performance dispersion-homogenizer, including the weight percentage content of each component and solid components.

| *Slurry* | *Binder (PUL) (%)* | *Plasticizer (Gly) (%)* | *C45 (%)* | *AC (%)* | *Solid content (%)* |
|---|---|---|---|---|---|
| sPUL-AC70 | 10 | 10 | 10 | 70 | 22.7 |
| sPUL-AC88 | 4 | 4 | 4 | 88 | 27 |
| sPUL-AC91 | 3 | 3 | 3 | 91 | 25 |

and with 10 wt%, 4 wt% and 3 wt% carbon black, labelled as sPUL-AC70, sPUL-AC88, and sPUL-AC91, respectively. The sPUL-AC70 formulation was selected as a benchmark, reflecting the state-of-the-art in literature. In all formulations containing PUL, glycerol (Gly) has been added as a plasticizer in the ratio PUL:glycerol equal to 1. Glycerol played the role of interacting with the PUL polymer chains decreasing the polymer's glass transition temperature ($T_g$), thereby enhancing its flexibility and toughness [32].

Each slurry was then used to prepare electrodes via *doctor blade* casting onto a carbon-coated aluminium current collector. This substrate was selected to enhance the adhesion between the active material and the current collector, a critical factor for electrode integrity. After drying, the resulting laminates were examined to evaluate cohesion among active material particles and adhesion to the current collector.

The main objective of this optimization stage was to increase the AC content—targeting the industrially relevant range of 87–95 wt%—while reducing the binder fraction, without compromising slurry processability or electrode integrity. Starting from the reference sPUL-AC70 (AC 70 wt %, PUL-Gly 20 wt %, C45 10 wt %) [21], several compositions were tested to identify the most promising formulation for scale-up. Among them, sPUL-AC88 (AC:PUL-Gly:C45, 88:8:4) demonstrated the best balance between viscosity, homogeneity, castability, and mechanical robustness of the resulting laminate, as will be discussed later.

This formulation was further processed by increasing the total solids content to enhance productivity. Attempts to increase the solid content further revealed some limitations: at 29 wt% total solid content, cast with a 250 μm blade, leading to ~10 mg $cm^{-2}$ mass loading, the mixing became more difficult and delamination was observed upon cutting the dried electrodes. Specifically, sPUL-AC91 exhibited poor edge integrity, with small cracks and broken pieces at the borders, likely due to the insufficient binder content. This behavior was attributed to a lack of cohesion and reduced adhesion to the current collector. Nevertheless, all other compositions listed in Table 1 produced uniform, crack-free laminates with good overall quality.

Building on the lab-scale findings, the most promising formulation (sPUL-AC88) was scaled up using a high-speed mixer, increasing the total solid content to 20 g to simulate conditions closer to pilot-scale manufacturing. For comparison, the reference formulation (sPUL-AC70) was also scaled up under the same conditions. These formulations are referred to as dPUL-AC88 and dPUL-AC70, respectively, and their compositions and solid-to-liquid ratios are summarized in Table 2.

The resulting slurries were cast onto carbon-coated aluminium foil using a *doctor blade*, producing larger-scale electrode laminates that were subsequently dried and analyzed. The morphology, cohesion, and adhesion of these electrodes were assessed via SEM and mechanical testing. Fig. 1 shows representative cross-sections and surface views of the electrodes. Laminates with AC content up to 88 wt% displayed homogeneous surfaces and strong contact with the current collector, with no visible defects or delamination. In contrast, laminates made from the 91 wt% AC slurry—though technically castable—exhibited microcracks and partial separation lines, indicating compromised cohesion due to the reduced binder fraction.

To further evaluate the mechanical robustness of the electrodes and their adhesion to the current collector, bending tests were performed on dPUL-AC70 and dPUL-AC88 laminates. This test is designed to simulate the final stage of the electrode manufacturing process, in which the dried electrode (represented by the dried slurry coated on an aluminium foil) is rolled at RT. Under these conditions, the deposited material must retain its integrity and adhere to the current collector without delaminating and cracking. Therefore, the bending test at RT provides a valuable indication of the electrode's mechanical stability during the final manufacturing step. The setup included a dedicated bending instrument equipped with height-adjustable rollers and a sliding vice to firmly secure the samples, ensuring consistent and controlled bending around mandrels with progressively decreasing diameters (Fig. 2). These tests allowed for a precise assessment of elasticity, adhesion, and elongation properties under mechanical stress. Both electrodes, cast onto carbon-coated aluminium foil using *doctor blade* and prepared via upscaled mixing, exhibited similar dry thicknesses (98 μm for dPUL-AC70 and 105 μm for dPUL-AC88). After each bending, the samples were analyzed using optical microscopy to detect the appearance of cracks or delamination. The results demonstrated that both formulations, regardless of the binder content, maintained excellent mechanical integrity. No visible defects were observed until the mandrel diameter was reduced below 2 mm. Even under these extreme bending conditions, the cracks observed were thin and did not lead to delamination from the current collector. These findings confirmed the high flexibility, cohesion, and adhesion of the electrodes, and validated the dPUL-AC88 formulation (AC:PUL-Gly:C45, 88:8:4) as suitable for further processing and integration into pouch cells. The successful scaling up of this formulation, combined with its robust mechanical performance, highlights its potential for real-device applications in sustainable, water-processable supercapacitors.

**Table 2**
Formulations of slurries with 20 g of solids (C45 and AC) prepared by high-speed mixer, including the weight percentage content of each component and the solid components.

| *Slurry code* | *Binder (PUL) (%)* | *Plasticizer (Gly) (%)* | *C45 (%)* | *AC (%)* | *Solid content (%)* |
|---|---|---|---|---|---|
| dPUL-AC70 | 10 | 10 | 10 | 70 | 23.2 |
| dPUL-AC88 | 4 | 4 | 4 | 88 | 29 |

### 3.2. Lab-scale cell assembly and electrochemical evaluation

To further assess the influence of electrode composition on electrochemical performance, a comparative study was carried out using electrodes prepared from lab-scale slurries (2 g total solids) mixed via rotor–stator homogenization. At first, a preliminary electrochemical investigation was conducted using electrochemical impedance spectroscopy (EIS), cyclic voltammetry (CV), and galvanostatic charge–discharge (GCD) tests in symmetric Swagelok cells with Whatman separator. The measurements were performed with 1 M $Et_4NBF_4$ in acetonitrile (ACN) as the electrolyte, and different PUL-based electrodes. The aim was to evaluate how variations in the content of PUL-Gly (binder/plasticizer) and conductive carbon (C45) affected the electrochemical response when increasing the AC fraction. Although a wide range of formulations was tested, this section focuses on three representative cases to ensure a concise yet informative discussion: the reference formulation with the lowest AC content (PUL-AC70), the formulation with the highest AC content (PUL-AC91), and the optimized intermediate composition (PUL-AC88), which showed the best compromise between mechanical stability and AC content. Symmetric EDLC cells were assembled in Swagelok configuration using these electrode laminates and tested under the same conditions to allow direct comparison. Table 3 summarizes the key characteristics of the selected cells, including the cell code, the dry electrode thickness and EDLCs total (2-electrodes) mass loading.

Fig. 3a reports the Nyquist plots from EIS tests of the three EDLCs with different PUL-based electrode formulations, before and after being subjected to CV and GCPL testing in 1M $Et_4NBF_4$ ACN electrolyte. Changes in the impedance spectra indicate how the internal resistance, capacitance, and overall electrochemical characteristics of cells evolve. ESR is evaluated as the sum of the resistances from the bulk electrolyte, the electrode, and the contact resistance between the electrode and the current collector (see SI and Fig. S1). Among the tested devices, S-sPUL-AC91 exhibited the lowest ESR (1.33 Ω $cm^2$), followed by S-sPUL-AC70 (1.40 Ω $cm^2$) and S-sPUL-AC88 (1.39 Ω $cm^2$). The lower ESR of S-sPUL-AC91 is primarily due to: i) the thinner electrode thickness, which

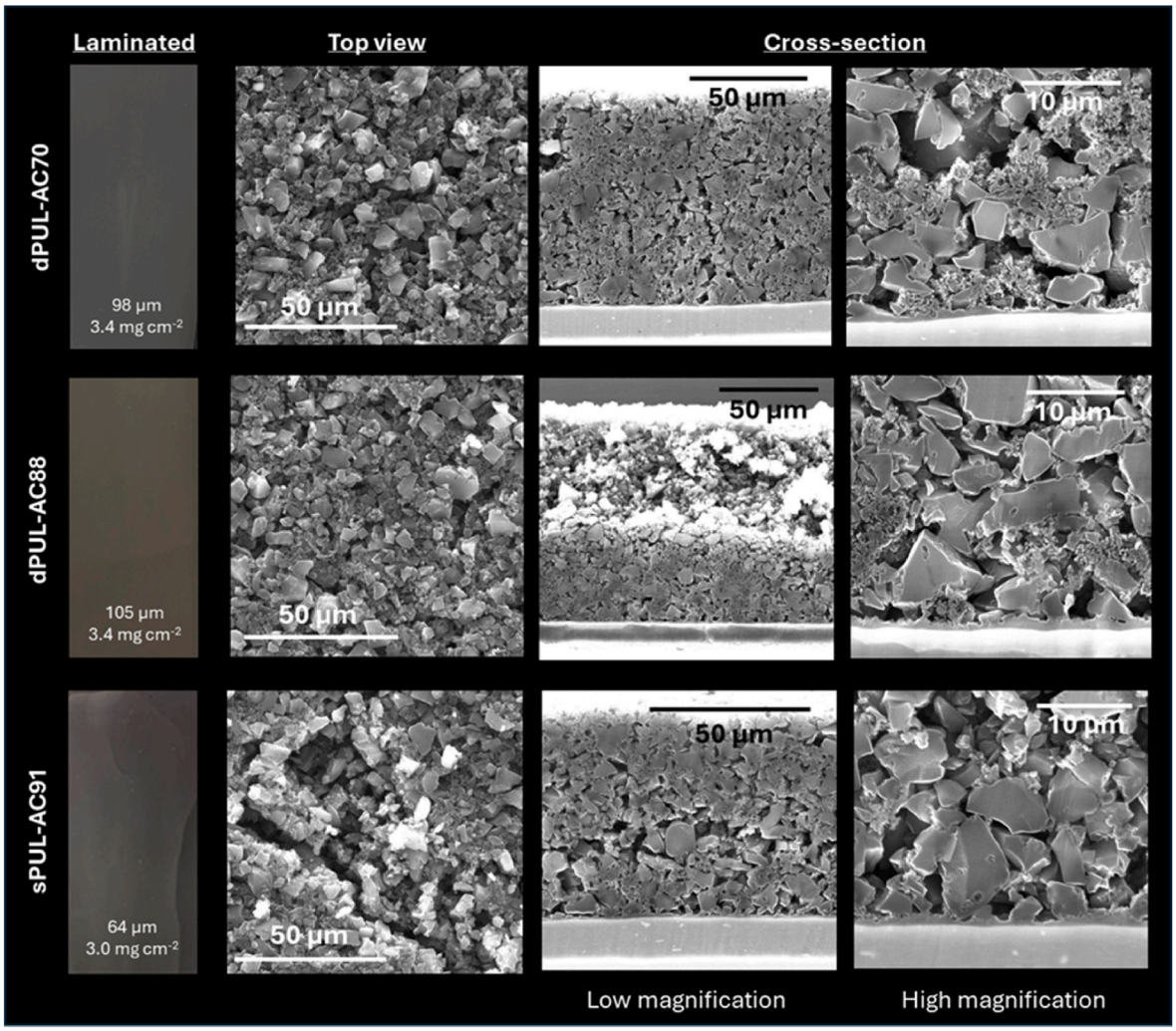


**Fig. 1.** SEM images of selected laminates observed at the surface (top-view) and at the cross-section: (a) dPUL-AC70 with composition of AC:PUL-Gly:C45 (70:20:10), (b) dPUL-AC88 with composition of AC:PUL-Gly:C45 (88:8:4) and (c) sPUL-AC91 prepared at lab-scale with composition of AC:PUL-Gly:C45 (91:6:3).

reduces the electronic pathway resistance, and ii) the lower amount of electronically insulating binder. This also confirms that reducing the carbon content while increasing the binder proportion leads to higher internal resistance, as expected. However, a higher binder content (20 wt%) in S-sPUL-AC70 resulted in a complete semicircle on the Nyquist plot, rather than the partial semicircles observed for S-sPU-AC88 and S-sPU-AC91. This probably indicates higher electrolyte resistance within the pores and greater contact resistance between the electrode and current collector [33]. Conversely, the device with the highest AC content (S-sPU-AC91) showed a broader in-pore resistance ($R_{INP}$) compared to the devices with 70 wt% and 80 wt% carbon, indicating a slower electrolyte diffusion within the carbon pores. This is also reflected in higher imaginary part of the impedance at lower frequencies, indicating a lower capacitance. Indeed, S-sPUL-AC88 showed the highest specific capacitance (21 F $g^{-1}$) compared to the S-sPUL-AC70 (19 F $g^{-1}$), and S-sPUL-AC91 (18 F $g^{-1}$). The fact that, despite its higher carbon content and lower ESR, S-sPUL-AC91 exhibits the lowest specific capacitance, can be explained by the inferior ion and electron percolation within the electrode, likely due to poor particle-particle and particle-current collector adhesion. This hypothesis is supported by the morphological analysis (Fig. 1), which clearly shows the presence of cracks and reduced homogeneity in the S-sPUL-AC91 electrode. These morphological features limit both the effective utilization of the active material and the efficient transport of charge carriers, ultimately reducing the electrochemical performance. In contrast, S-sPUL-AC88, although slightly thicker and exhibiting higher ESR, benefits from a more homogeneous structure with improved interfacial contact and better connectivity within the electrode. This results in significantly higher capacitance values, despite the slightly lower carbon content.

No significant differences can be detected by comparing the Nyquist plots recorded before and after the CV and GCPL tests (Fig. 3a and 3b), indicating that the cells were well assembled and the wetting time appropriate.

The voltammograms of all the EDLCs at 50 mV $s^{-1}$ in Fig. 3c feature the typical rectangular shape expected for a pure capacitive response. Fig. 3d reports the GCPL results profiles at 10 A $g^{-1}$ that indicate a very low ohmic drop within a discharge time of 4–5 s. Fig. 3e reports the EDLC specific capacitance, evaluated from the GCPL discharges at different currents, which are also reported in Table S1. It is important to note that the specific capacitance is calculated considering the total mass of the two electrodes, contrary to what is usually reported in the literature, where only the active mass is typically considered and non-active components (binder and carbon additive) are neglected. The cell with the highest AC content (91 wt%) shows the lowest specific capacitance (20 F $g^{-1}$ at 0.25 A $g^{-1}$ and 18 F $g^{-1}$ at 10 A $g^{-1}$), with a pronounced decay in capacitance between 0.1 and 2 A $g^{-1}$. The device with 88 wt% AC exhibits the highest specific capacitance (22 F $g^{-1}$ at 0.25 A $g^{-1}$), with a slight decrease at low specific current, remaining quite stable after 1 A $g^{-1}$, with a specific capacitance of 21 F $g^{-1}$ at 10 A $g^{-1}$.

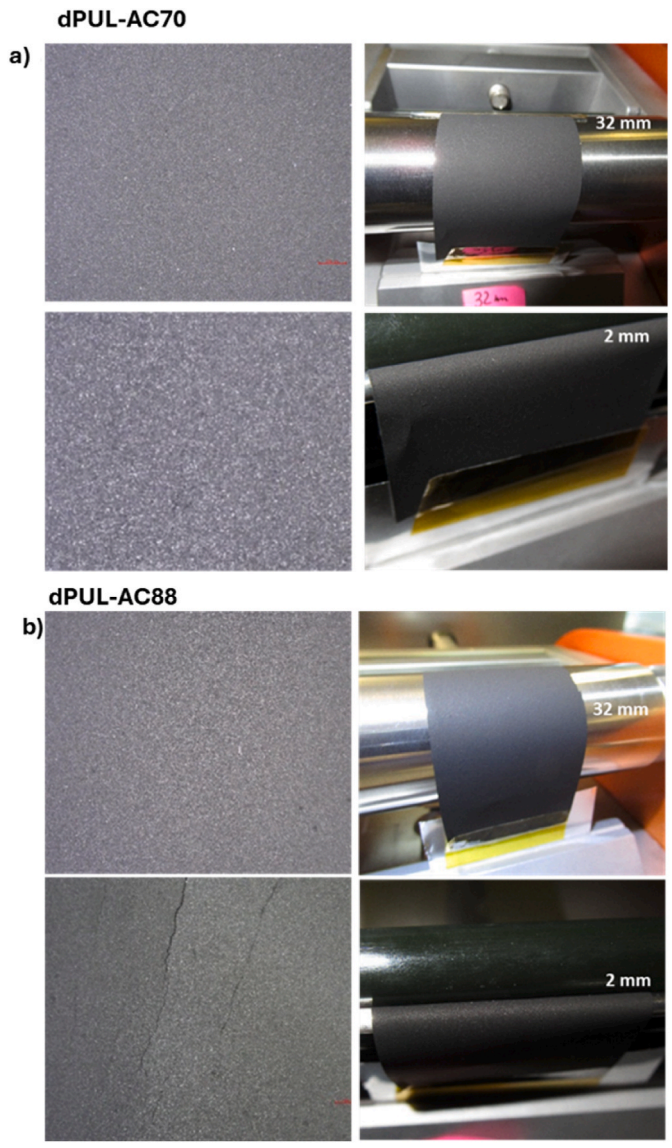


**Fig. 2.** Bending test performed on (a) dPUL-AC70 and (b) dPUL-AC88 electrodes on similar dry thicknesses 98 μm, and 105 μm. In particular, it is reported the microscope analysis before the bending, the starting bending with 32 mm mandrels and the microscope analysis together with the respective bending when the first crack appears to the electrode.

**Table 3**
Cell code, electrode formulation and thickness, and EDLCs total (2-electrodes) mass loading of the Swagelock cells (S) assembled with PUL-based electrodes, 1 M $Et_4NBF_4$ -ACN electrolyte and Whatman separator.

| Cell code | Electrode formulation AC:PUL-Gly:C45 | Thickness (μm) | EDLCs total electrode mass loading (mg $cm^{-2}$) |
|---|---|---|---|
| S-sPUL-AC70 | 70:20:10 | 100 | 9.3 |
| S-sPUL-AC88 | 88:8:4 | 110 | 6.6 |
| S-sPUL-AC91 | 91:6:3 | 130 | 6.6 |

Finally, the energy and power density values of the different cells were evaluated at different constant currents and at RT. The results are presented in the Ragone plots in Fig. 3f while values are reported in Table S2. These plots compare the specific energy and power of the cells based on the total mass of the two electrodes. The S-sPUL-AC88 cell demonstrates the best performance in terms of both specific energy (22.4 Wh $kg^{-1}$ at 0.25 A $g^{-1}$ within a discharge time of 240 s and 19.4 Wh $kg^{-1}$ at 10 A $g^{-1}$ within a discharge time of 5 s) and power (0.3 W $kg^{-1}$ at 0.25 A $g^{-1}$ 12.9 W $kg^{-1}$ at 10 A $g^{-1}$). The EDLC S-sPUL-AC91 with the highest AC content features the worst performance because of the lower quality of the electrodes that provided higher internal resistance (19.9 Wh $kg^{-1}$ and 0.3 W $kg^{-1}$ at 0.25 A $g^{-1}$). S-sPUL-AC70 performs well (20.0 Wh $kg^{-1}$ and 0.2 W $kg^{-1}$ at 0.25 A $g^{-1}$), but worse than S-sPUL-AC88, which has a higher AC content and a lower binder amount.

Considering these results, the electrode formulation AC:PU-Gly:C45 at 88:8:4 was selected as the most suitable for upscaling the device manufacturing. The following section reports the results obtained using this formulation, but in a pouch cell configuration.

### 3.3. Pouch cell assembly and electrochemical evaluation

Pouch cells were assembled using the dPUL-AC88 electrodes and an electrospun PUL membrane as separator (Fig. 4), aiming to demonstrate the feasibility of a fully aqueous-based process. To investigate the influence of the electrolyte solvent on device performance and safety, two different electrolyte formulations were tested: 1 M $Et_4NBF_4$ - acetonitrile in the cell P-dPUL-ACN and 1 M $Et_4NBF_4$ - propylene carbonate for the EDLC P-dPUL-PC. While $Et_4NBF_4$-ACN is widely used for its high ionic conductivity (56 mS $cm^{-1}$at RT), $Et_4NBF_4$-PC is appealing for its low volatility and flammability, making it a safer and more sustainable alternative to the ACN-based electrolyte for practical applications, despite its lower conductivity (15 mS $cm^{-1}$ at RT). Table S3 reports the key characteristics of the assembled cells, including the cell code, the EDLCs mass and EDLCs total (2-electrodes) mass loading that was 9.0–9.4 mg $cm^{-2}$, and the respective electrolyte.

Thermogravimetric analysis and differential scanning calorimetry of electrospun PUL have been previously reported [30] and demonstrated that PUL fibers have an extensive temperature range of applicability because their morphology is maintained up to 250 °C, after which the material starts to thermally degrade. Fig. S2 shows that the dimensional stability of the membrane is preserved up to 250 °C. Stress-strain tensile tests (Fig. S3) allowed to determine the mechanical properties of the membrane which displays a Young's modulus of 71 (±5) MPa, stress at break of 2 (±0.2) MPa, and deformation at break of 10 (±2) %. Contact angles, measured by using the electrolytes as liquid phase, highlight that both electrolytes fully penetrate the pores of the PUL membranes within 0.5 s and 2 s in the case of ACN- and PC-based electrolyte, respectively (Fig. S4). In addition, PUL electrospun membrane did not show any deformation or swelling under prolonged contact with both electrolytes 1 M $Et_4NBF_4$-ACN and 1 M $Et_4NBF_4$-PC used in this work (Fig. S5). Overall, these characterizations support the use of PUL membrane as suitable EDLC separator [30].

Fig. 5 presents the resutls of the electrochemical characterizations of the different pouch cells tested. The Nyquist plots in Fig. 5a reveal a notable reduction in internal resistance with an ESR of 1.2 Ω $cm^2$ using 1M $Et_4NBF_4$ - ACN in P-dPUL-ACN compared to 2.4 Ω $cm^2$ for P-dPUL-PC that features the PC solution. This difference is directly linked to the ionic conductivity of the respective electrolytes, reflecting the lower viscosity and higher ion transport rates in ACN-based cells [34]. The lower conductivity of $Et_4NBF_4$ - PC also explains the larger diameter of the high-frequency semicircle that depicts the in-pore resistance $R_{INP}$.

The cyclic voltammetry analysis at 50 mV $s^{-1}$ (see Fig. 5b) reveals a purely capacitive behaviour, which is indicative of the high quality of the assembled pouch cells. The rate response of the EDLCs was also investigated. Fig. 5c and Table S4 show the trend of the specific capacitance at different currents. P-dPUL-PC demonstrates competitive performance with respect to the ACN-based cell at almost all applied specific currents. Indeed, the device retained ca. 20 F $g^{-1}$ up to 10 A $g^{-1}$. Only beyond 25 A $g^{-1}$ P-dPUL-ACN outperformed P-dPUL-PC, highlighting the impact of electrolyte formulation on EDLC performance,

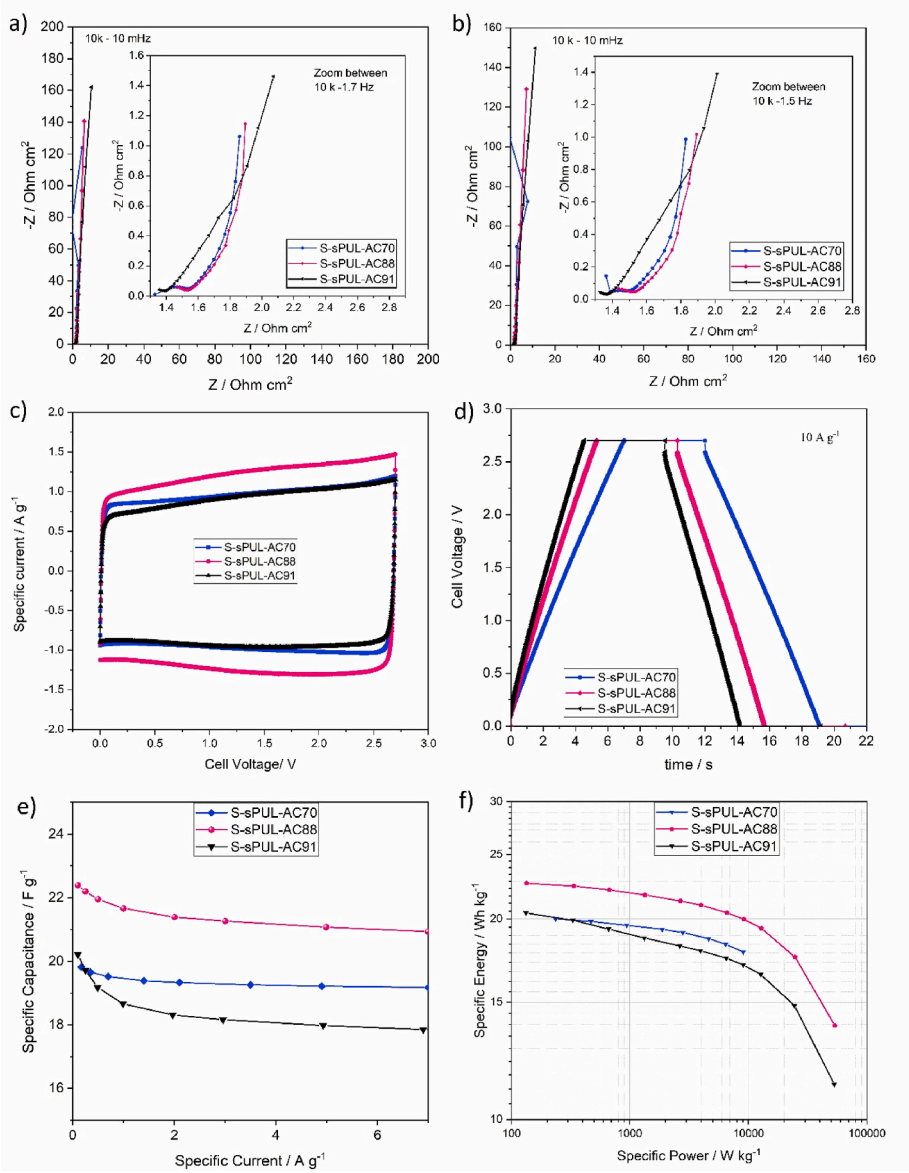


**Fig. 3.** Electrochemical results of the Swagelok cells S-sPUL-AC70, S-sPUL-AC88 and S-sPUL-AC91 with AC:PUL-Gly:C45 (70:20:10, 88:8:4, 91:6:3) electrodes, respectively, 1M $Et_4NBF_4$ ACN electrolyte and Whatman separator. Nyquist plots from EIS (a) before and (b) after CV and GCPL tests; (c) CVs at 50 mV $s^{-1}$, (d) GCPL charge/discharge profiles at 10 A $g^{-1}$, (e) trends of specific capacitance and (f) Ragone plot from GCPL at different currents with cut-off voltage 0.0 V–2.7 V.

especially at very high rates (Fig. S6). As it can be observed in the GCPL profiles reported in Fig. 5c, at 1 A (5 A $g^{-1}$) both systems exhibit the same charge-discharge profile, with a discharge time of 7s. Hence, the use of $Et_4NBF_4$ - ACN is advantageous only in applications where discharge times are shorter than 5 s.

Fig. 6a reports the Ragone Plots obtained by the analyses of the GCPL tests and the data reported in Table S5. The Figure highlights how different electrolytes influence the energy-to-power performance of each of the systems. At the lowest power rates (1 kW $kg^{-1}$) the two EDLCs deliver similar specific energy of ca 20 Wh $kg^{-1}$. However, at the higher current rates the ACN-based EDLC is superior in both power and energy densities, achieving 12.0 kW $kg^{-1}$ and 16.4 Wh $kg^{-1}$ at 3 A. At 3 A, the PC-based EDLC system delivers 10.3 kW $kg^{-1}$ and 16.5 Wh $kg^{-1}$.

The durability of EDLCs is a key metric that needs to be evaluated for any kind of system validation. Since well-engineered systems can cycle over hundreds of thousands of cycles, we performed accelerated ageing by floating tests at RT followed 60 °C. Fig. 6b reports the trend of the capacitance (normalized to the value exhibited at the first cycle) evaluated by the discharge step during subsequent floating. The Figure shows that P-dPUL-ACN has exceptional capacitance retention over 1000 h, maintaining more than 80 % of its initial capacitance after the first 10 h needed to stabilize the system (see Fig. S6). Instead, when PC-based electrolyte was used, capacitance retention dropped below 80 % after 450 h. Interestingly, the floating tests conducted at 60 °C (after those at RT) showed the opposite trend. P-dPUL-PC featured a higher specific capacitance retention over 1000 h compared to P-dPUL-ACN. In particular, after 1000 h, the increase of temperature resulted in the decrease of the P-dPUL-ACN specific capacitance by 20 %, from 20 F $g^{-1}$ to 16 F $g^{-1}$. Instead, in the case of P-dPUL-PC, the temperature rise provided an increase of capacitance by 20 % and, after additional 1000 h (total 2000 h), the overall capacitance loss was only 10 %. This is probably due to the fact that $Et_4NBF_4$ - PC has a higher viscosity and lower ionic conductivity than $Et_4NBF_4$ - ACN [35,36]. Indeed, the temperature increase enhances reaction kinetics and EDLC capacitance, suggesting that $Et_4NBF_4$ - PC is more suitable for high temperature operation EDLCs. Overall, both EDLCs demonstrate very good capacitance retention, highlighting the long operating life of the proposed devices.

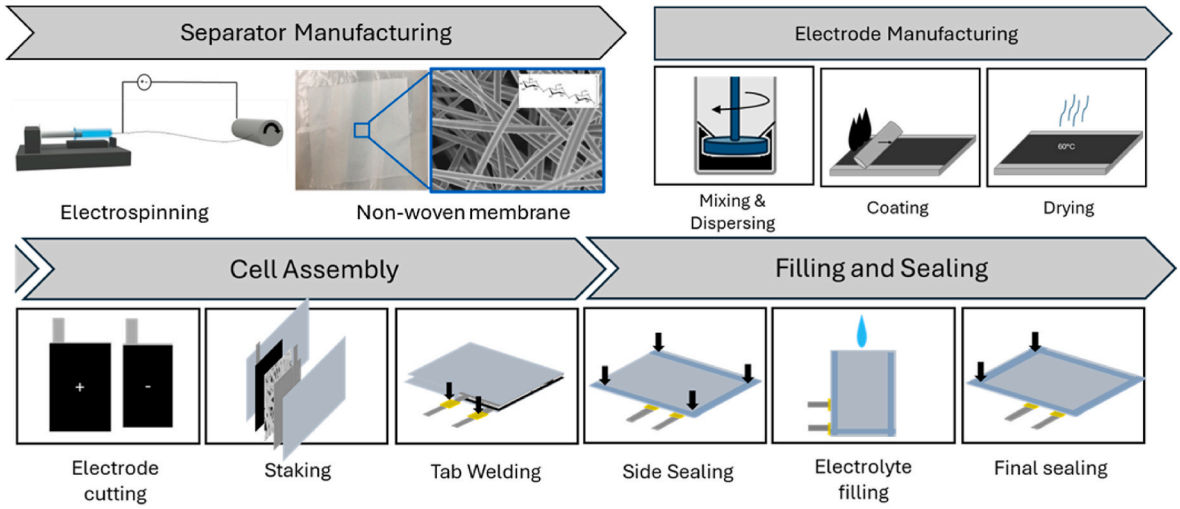


**Fig. 4.** Production process of PUL membrane and pouch cell assembling.

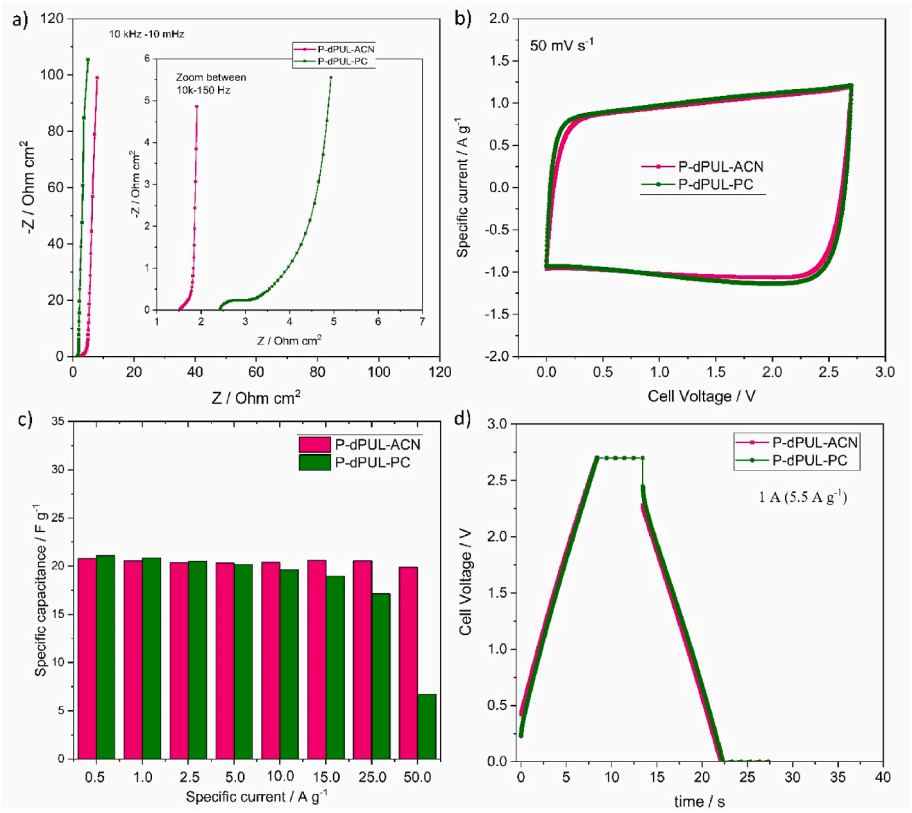


**Fig. 5.** (a) Nyquist plots (b) CVs at 50 mV $s^{-1}$, (c) trends of specific capacitance evaluated by GCPL at different specific currents, (d) GCPL charge/discharge profiles at 1 A (5 A $g^{-1}$) and RT of the pouch cells with PUL-electrodes, PUL-separator and ACN or PC-based electrolyte.

To contextualize the performance of our devices, Table 4 presents a comparison of the performance of the top-performing PUL-based (SC) from this work with selected examples from recent literature, focusing on studies published within the last five years. This table aims to provide a comprehensive overview of the current state of the art (SoA) in the field, acknowledging that direct comparisons between studies are difficult due to differences in experimental conditions and electrode formulations. The comparison highlights that the results from this work are within the capacitance and energy density range of the SoA, while exceeding previous studies in terms of cycling stability.

## 4. Conclusions

In this study, the feasibility of manufacturing sustainable and high-performance supercapacitor pouch cells on a large scale, using water-processable materials for both the electrodes and the separator has been demonstrated. PUL has been employed as a versatile dual-role polymer, working both as binder and separator. As a binder, it enables a scalable manufacturing process that provides excellent mechanical integrity of fabricated electrodes. The optimized electrode formulation (AC:PU-Gly:C45, 88:8:4) enabled uniform, crack-free laminates with a high solid content (up to 88 wt %) and single electrode mass loading

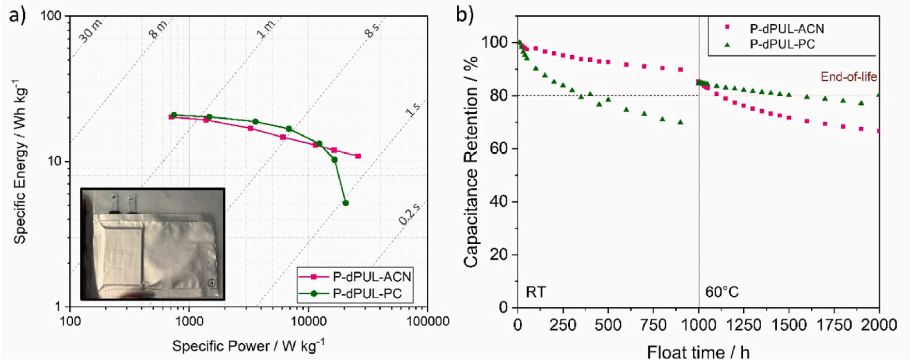


**Fig. 6.** (a) Ragone plots calculated from GCPL at different currents with cut-off voltage 0.0–2.7 V and (b) Capacitance retention under floating tests of pouch cells with PUL-electrodes, PUL-separator and ACN or PC-based electrolyte.

**Table 4**
Comparison of selected studies from the last five years using different polymers as binders.

| Binder | Electrode Formulation | Electrolyte | Specific capacitance (F $g^{-1}$) | Max. Energy Density (kWh $kg_{AM}^{-1}$) | Max. Power Density (W $kg_{AM}^{-1}$) | Cycling Stability | Reference |
|---|---|---|---|---|---|---|---|
| ***Pullulan (PUL) – HBLME***[a] | AC (70 wt%)/CB (10 wt %)/PUL-Gly (20 wt%) | EmimTFSI (IL) | 15.9 (at 50 mV $s^{-1}$) | 19.6 | 4.6 | ~90 % after 2000 cycles | [19] |
| ***Pullulan (PUL) – LBHME***[a] | AC (85 wt%)/CB (5 wt%)/PUL-Gly (10 wt%) | EmimTFSI (IL) | 6.2 (at 50 mV $s^{-1}$) | 7.2 | 3.7 | ~77 % after 5000 cycles | [19] |
| ***CMC:SBR*** | AC (85 wt%)/CB (5 wt %)/CMC:SBR (10 wt%) | 1M $Et_4NBF_4$ (ACN) | 22.9 (at 5 A $g^{-1}$) | 24.4 | 25.5 | – | [18] |
| ***Epoxy:amine (E:A0.5)*** | AC (85 wt%)/CB (5 wt %)/Epoxy:amine (10 %) | 1M $Et_4NBF_4$ (ACN) | 16.8 (at 5 A $g^{-1}$) | 18.3 | 21.5 | – | [18] |
| ***Polyurethane (PU-H)*** | AC (85 wt%)/CB (5 wt %)/Polyurethane (10 wt%) | 1M $Et_4NBF_4$ (ACN) | 26.7 (at 5 A $g^{-1}$) | 26.2 | 25.8 | ~98 % after 2500 cycles | [18] |
| ***Chitosan*** | AC (85 wt%)/CB (10 wt %)/Chitosan (5 wt%) | 1.5M $Na_2SO_4$ (aq) | 18.8 (at 5 A $g^{-1}$) | – | – | ~93,4 % after 5000 cycles | [37] |
| ***Potato starch:guar gum*** | AC (90 wt%)/CB (5 wt%)/PS:GG (5 wt%) | 1M $Et_4NBF_4$ (PC) | 25 (at 5 A $g^{-1}$) | – | – | – | [38] |
| ***Potato starch:CMC (PS50/CMC50)*** | AC (93 wt%)/CB (2.8 wt%)/PS:CMC (4.2 wt%) | 1M $Pyr_{14}BF_4$ (ACN) | – | – | – | ~80 % after 250h | [4] |
| ***Xanthan gum:CMC (XG50/CMC50)*** | AC (93 wt%)/CB (2.8 wt %)/XG:CMC (4.2 wt%) | 2M $Pyr_{11}BF_4$ (ACN) | – | – | – | ~75 % after 500h | [4] |
| ***Pullulan (PUL)*** | AC (88 wt%)/CB (4 wt%)/PUL-Gly (8 wt%) | 1M $Et_4NBF_4$ (ACN) | 20.6 (at 5 A $g^{-1}$) | 20.3 | 26.2 | ~90 % after 500h (pouch cell) | This work |

EmimTFSI: 1-Ethyl-3-methylimidazolium bis(trifluoromethylsulfonyl)imide; IL: ionic liquid; $Pyr_{14}BF_4$: 1-Butyl-1-methylpyrrolidinium tetrafluoroborate.
[a] CB: carbon black; HBLME: high binder low mass electrode; LBHME: low binder high mass electrode.

higher than 5 mg $cm^{-2}$, suitable for industrial-scale applications. These electrodes, combined with electrospun PUL membrane separators, provide a fully water-processed EDLC. Moreover, electrochemical performance was validated in 4 F- pouch cells (20 $cm^2$, 10 mg $cm^{-2}$) with two different electrolytes: 1M $Et_4NBF_4$ in ACN or in the greener PC. The comparison highlights the critical role of the electrolyte in device performance and durability. ACN-based cells exhibited lower internal resistance and superior power and energy at specific currents > 10 A $g^{-1}$ and RT. On the other hand, PC-based systems, achieved competitive specific capacitance values of 21 F $g^{-1}$ at the lowest currents. In terms of durability, floating tests confirmed the long-term stability of ACN-based pouch cells, retaining over 80 % of their initial capacitance after 1000 h. Although PC-based cells exhibited a faster capacitance decline at RT (retaining stability for approximately 450 h), at 60 °C it outperformed the cell with ACN, therefore emerging as a promising alternative for safe, high-temperature operation. In addition, a lower toxicity and enhanced safety profile, make PC-based cells attractive for applications prioritizing environmental sustainability. Overall, the results underscore the viability of integrating water-processable PUL-based electrodes and separators with the sustainable PC-based electrolyte for scalable energy storage applications. This approach represents a significant step forward in the development of environmentally friendly, high-performance EDLCs.

## CRediT authorship contribution statement

**Elisabetta Petri:** Writing – review & editing, Writing – original draft, Visualization, Methodology, Investigation, Formal analysis, Data curation, Conceptualization. **Maria Arnaiz:** Writing – review & editing, Writing – original draft, Visualization, Validation, Supervision, Resources, Investigation, Data curation, Conceptualization. **Chiara Gualandi:** Writing – review & editing, Writing – original draft, Resources, Conceptualization. **Francesca Soavi:** Writing – review & editing, Writing – original draft, Visualization, Validation, Supervision, Investigation, Funding acquisition, Formal analysis, Conceptualization. **Jon Ajuria:** Writing – review & editing, Writing – original draft, Visualization, Validation, Supervision, Resources, Methodology, Funding acquisition, Conceptualization.

## Declaration of competing interest

The authors declare the following financial interests/personal relationships which may be considered as potential competing interests: Francesca Soavi reports financial support was provided by European Commission. If there are other authors, they declare that they have no known competing financial interests or personal relationships that could have appeared to influence the work reported in this paper.

## Acknowledgements

E. P. and F.S. acknowledge the support by the European Union within the Horizon 2020 Research and Innovation Program 2020–2023 (Grant No. 963550 HyFlow project https://hyflow-h2020.eu/). F.S: acknowledges MOST - Sustainable Mobility Centre project, funded by the European Union Next-Generation EU (PIANO NAZIONALE DI RIPRESA E RESILIENZA (PNRR) and MISSIONE 4 COMPONENTE 2, INVESTIMENTO 1.4 e D.D. 1033 June 17, 2022, CN00000023). M.A. and J.A. acknowledge the Basque Government for the ELKARTEK 2023 call (project CICe2023) under the application number KK-2023/00063.

## Appendix A. Supplementary data

Supplementary data to this article can be found online at https://doi.org/10.1016/j.jpowsour.2025.238177.

## Data availability

Data will be made available on request.

## References

[1] P. PbSO, N. Koh, -e -, V. Li Si, S. LiX Building better batteries, Nature 451 (7179 451) (2008) 652–657, https://doi.org/10.1038/451652a, 2008.
[2] I. Hadjipaschalis, A. Poullikkas, V. Efthimiou, Overview of current and future energy storage technologies for electric power applications, Renew. Sustain. Energy Rev. 13 (2009) 1513–1522. https://ideas.repec.org/a/eee/rensus/v13y2009i6-7p1513-1522.html. (Accessed 14 February 2025).
[3] A.G. Pandolfo, A.F. Hollenkamp, Carbon properties and their role in supercapacitors, J. Power Sources 157 (2006) 11–27, https://doi.org/10.1016/J.JPOWSOUR.2006.02.065.
[4] L. Köps, P. Ruschhaupt, C. Guhrenz, P. Schlee, S. Pohlmann, A. Varzi, S. Passerini, A. Balducci, Development of a high-energy electrical double-layer capacitor demonstrator with 5000 F in an industrial cell format, J. Power Sources 571 (2023) 233016, https://doi.org/10.1016/J.JPOWSOUR.2023.233016.
[5] Y.K. Lee, The effect of active material, conductive additives, and binder in a cathode composite electrode on battery performance, Energies 12 (2019) 658, https://doi.org/10.3390/EN12040658.
[6] N.A. Salleh, S. Kheawhom, N. Ashrina A Hamid, W. Rahiman, A.A. Mohamad, Electrode polymer binders for supercapacitor applications: a review, J. Mater. Res. Technol. 23 (2023) 3470–3491, https://doi.org/10.1016/J.JMRT.2023.02.013.
[7] D. Bresser, D. Buchholz, A. Moretti, A. Varzi, S. Passerini, Alternative binders for sustainable electrochemical energy storage – the transition to aqueous electrode processing and bio-derived polymers, Energy Environ. Sci. 11 (2018) 3096–3127, https://doi.org/10.1039/C8EE00640G.
[8] D.L. Wood, J.D. Quass, J. Li, S. Ahmed, D. Ventola, C. Daniel, Technical and economic analysis of solvent-based lithium-ion electrode drying with water and NMP, Dry. Technol. 36 (2018) 234–244, https://doi.org/10.1080/07373937.2017.1319855.
[9] D.E. Malek, L.A. Malley, T.W. Slone, G.S. Elliott, G.L. Kennedy, W. Mellert, K. Deckardt, C. Gembardt, B. Hildebrand, S.R. Murphy, D.B. Bower, G.A. Wright, Repeated dose toxicity study (28 days) in rats and mice with N-methylpyrrolidone (NMP), Drug Chem. Toxicol. 20 (1997) 63–77, https://doi.org/10.3109/01480549709011079.
[10] L. Kp, C. Nc, C. R, B. JR, S. Pw, Toxicity of N-methyl-2-pyrrolidone (NMP): teratogenic, subchronic, and two-year inhalation studies, Fund. Appl. Toxicol. 9 (1987) 222–235, https://doi.org/10.1016/0272-0590(87)90045-5.
[11] W. Zhu, D.R. Schmehl, C.A. Mullin, J.L. Frazier, Four common pesticides, their mixtures and a formulation solvent in the hive environment have high oral toxicity to Honey Bee Larvae, PLoS One 9 (2014) e77547, https://doi.org/10.1371/JOURNAL.PONE.0077547.
[12] F.M. Courtel, S. Niketic, D. Duguay, Y. Abu-Lebdeh, I.J. Davidson, Water-soluble binders for MCMB carbon anodes for lithium-ion batteries, J. Power Sources 196 (2011) 2128–2134, https://doi.org/10.1016/j.jpowsour.2010.10.025.
[13] T.S. Poet, C.R. Kirman, M. Bader, C. Van thriel, M.L. Gargas, P.M. Hinderliter, Quantitative risk analysis for N-methyl pyrrolidone using physiologically based pharmacokinetic and benchmark dose modeling, Toxicol. Sci. 113 (2010) 468–482, https://doi.org/10.1093/TOXSCI/KFP264.
[14] K. Rollag, D. Juarez-Robles, Z. Du, D.L. Wood, P.P. Mukherjee, Drying temperature and capillarity-driven crack formation in aqueous processing of Li-Ion battery electrodes, ACS Appl. Energy Mater. 2 (2019) 4464–4476, https://doi.org/10.1021/ACSAEM.9B00704.
[15] A. Balducci, Electrolytes for high voltage electrochemical double layer capacitors: a perspective article, J. Power Sources 326 (2016) 534–540, https://doi.org/10.1016/J.JPOWSOUR.2016.05.029.
[16] P. Simon, Y. Gogotsi, Materials for electrochemical capacitors, Nat. Mater. 7 (11 7) (2008) 845–854, https://doi.org/10.1038/nmat2297, 2008.
[17] A. Bothe, A. Balducci, The impact of the thermal stability of non-conventional electrolytes on the behavior of high voltage electrochemical capacitors operating at 60 °C, Electrochim. Acta 374 (2021) 137919, https://doi.org/10.1016/J.ELECTACTA.2021.137919.
[18] M. Arnaiz, M. Fernandez, A. Suty, S. Martin-Fuentes, D. Carriazo, A. Bouvet-Marchand, A. Villaverde, M.C. Morant-Miñana, Novel binders for aqueous electrode processing of electrochemical capacitors, ChemSusChem (2024) e202401316, https://doi.org/10.1002/CSSC.202401316.
[19] G.E. Spina, F. Poli, A. Brilloni, D. Marchese, F. Soavi, Natural polymers for green supercapacitors, Energies 13 (2020) 3115, https://doi.org/10.3390/EN13123115.
[20] A. Brilloni, F. Poli, G.E. Spina, C. Samorì, E. Guidi, C. Gualandi, M. Maisuradze, M. Giorgetti, F. Soavi, Easy recovery of Li-ion cathode powders by the use of water-processable binders, Electrochim. Acta 418 (2022) 140376, https://doi.org/10.1016/J.ELECTACTA.2022.140376.
[21] F. Poli, D. Momodu, G.E. Spina, A. Terella, B.K. Mutuma, M.L. Focarete, N. Manyala, F. Soavi, Pullulan-ionic liquid-based supercapacitor: a novel, smart combination of components for an easy-to-dispose device, Electrochim. Acta 338 (2020) 135872, https://doi.org/10.1016/J.ELECTACTA.2020.135872.
[22] A. Brilloni, F. Marchesini, F. Poli, E. Petri, F. Soavi, Performance comparison of LMNO cathodes produced with Pullulan or PEDOT:PSS water-processable binders, Energies 15 (2022) 2608, https://doi.org/10.3390/EN15072608.
[23] E. Bel Hadj Jrad, F. Soavi, C. Dridi, Development of flexible and sustainable all quasi-solid-state supercapacitors based on ecofriendly binders on aluminum foil, J. Energy Storage 88 (2024) 111471, https://doi.org/10.1016/J.EST.2024.111471.
[24] S. Tabasum, A. Noreen, M.F. Maqsood, H. Umar, N. Akram, Z.i.H. Nazli, S.A. S. Chatha, K.M. Zia, A review on versatile applications of blends and composites of pullulan with natural and synthetic polymers, Int. J. Biol. Macromol. 120 (2018) 603–632, https://doi.org/10.1016/J.IJBIOMAC.2018.07.154.
[25] R.S. Singh, G.K. Saini, J.F. Kennedy, Pullulan: microbial sources, production and applications, Carbohydr. Polym. 73 (2008) 515–531, https://doi.org/10.1016/J.CARBPOL.2008.01.003.
[26] C.T. Chen, K.I. Chen, H.H. Chiang, Y.K. Chen, K.C. Cheng, Improvement on physical properties of Pullulan films by novel cross-linking strategy, J. Food Sci. 82 (2017) 108–117, https://doi.org/10.1111/1750-3841.13577.
[27] S. Chen, S. He, H. Hou, Electrospinning technology for applications in supercapacitors, Curr. Org. Chem. 17 (2013) 1402–1410, https://doi.org/10.2174/1385272811317130007.
[28] Global Top Page | Toshiba, (n.d.). https://www.global.toshiba/ww/top.html (accessed June 11, 2025).
[29] L. Persano, A. Camposeo, C. Tekmen, D. Pisignano, Industrial upscaling of electrospinning and applications of polymer nanofibers: a review, Macromol. Mater. Eng. 298 (2013) 504–520, https://doi.org/10.1002/MAME.201200290.
[30] C. Gualandi, A. Zucchelli, M. Fernández Osorio, J. Belcari, M.L. Focarete, Nanovascularization of polymer matrix: generation of nanochannels and nanotubes by sacrificial electrospun fibers, Nano Lett. 13 (2013) 5385–5390, https://doi.org/10.1021/NL402930X.
[31] A. Menichetti, F. Ramacciotti, G. Sciutto, M.L. Focarete, M. Montalti, S. Prati, C. Gualandi, Nanofibrous photothermal materials from natural resources: a green approach for artwork restoration, ACS Appl. Mater. Interfaces 16 (2024) 69829–69838, https://doi.org/10.1021/ACSAMI.4C14532/ASSET/IMAGES/LARGE/AM4C14532_0006.JPEG.
[32] P.R. Vuddanda, M. Montenegro-Nicolini, J.O. Morales, S. Velaga, Effect of plasticizers on the physico-mechanical properties of pullulan based pharmaceutical oral films, Eur. J. Pharmaceut. Sci. 96 (2017) 290–298, https://doi.org/10.1016/J.EJPS.2016.09.011.
[33] B.A. Mei, O. Munteshari, J. Lau, B. Dunn, L. Pilon, Physical interpretations of nyquist plots for EDLC electrodes and devices, J. Phys. Chem. C 122 (2018) 194–206, https://doi.org/10.1021/ACS.JPCC.7B10582/ASSET/IMAGES/LARGE/JP-2017-10582X_0009.JPEG.
[34] Q.G. Zhang, S.S. Sun, S. Pitula, Q.S. Liu, U. Welz-Biermann, J.J. Zhang, Electrical conductivity of solutions of ionic liquids with methanol, ethanol, acetonitrile, and propylene carbonate, J. Chem. Eng. Data 56 (2011) 4659–4664, https://doi.org/10.1021/JE200616T/SUPPL_FILE/JE200616T_SI_001.PDF.
[35] S. Pohlmann, A. Balducci, A new conducting salt for high voltage propylene carbonate-based electrochemical double layer capacitors, Electrochim. Acta 110 (2013) 221–227, https://doi.org/10.1016/J.ELECTACTA.2013.02.114.
[36] J. Krummacher, C. Schütter, S. Passerini, A. Balducci, Characterization of different conductive salts in ACN-based electrolytes for electrochemical double-layer capacitors, Chemelectrochem 4 (2017) 353–361, https://doi.org/10.1002/CELC.201600534;JOURNAL:JOURNAL:21960216;PAGE:STRING:ARTICLE/CHAPTER.
[37] L. Bargnesi, A. Rozzarin, G. Lacarbonara, S. Tombolesi, C. Arbizzani, Sustainable modification of Chitosan binder for capacitive electrodes operating in aqueous electrolytes, Chemelectrochem 10 (2023) e202201080, https://doi.org/10.1002/CELC.202201080;PAGE:STRING:ARTICLE/CHAPTER.
[38] P. Ruschhaupt, A. Varzi, S. Passerini, Natural polymers as green binders for high-loading supercapacitor electrodes, ChemSusChem 13 (2020) 763–770, https://doi.org/10.1002/CSSC.201902863.